Sequence-Selective Metalation of Double-Helical Oligodeoxyribonucleotides with Pt^{II}, Mn^{II}, and Zn^{II} Ions

J. Vinje,[a] J. A. Parkinson,[b] P. J. Sadler,[c] T. Brown,[d] and E. Sletten*[a]

Abstract: Reactions of $[PtCl(dien)]^+$ (dien = diethylenetriamine), Mn^{2+} and Zn^{2+} ions with three different double-helical oligodeoxyribonucleotides, which contain the central sequence GGXY (XY = AT, TA or CC) have been monitored by NMR spectroscopy. 2D [^{1}H, ^{15}N] HSQC/HMQC NMR spectroscopy using ^{15}N-labeled Pt(dien) shows that the rate of formation of 3′-G-N7 and 5′-G-N7 platinated adducts is highly sequence dependent. The relative rates of platination of 5′-G versus 3′-G are largest for the sequence -GGCC-, for which only a small fraction of the 3′-G adduct is formed; for -GGTA-, the rate of 5′-G platination is about eight times that of 3′-G, and for -GGAT- the ratio is 1.2. These values are in qualitative agreement with those obtained for G-N7/Mn^{2+} selectivity as determined by paramagnetic line broadening of the adjacent G-H8, and also G-N7/Zn^{2+} selectivity as determined by G-H8 chemical shift changes. Fluctuation in the nucleophilicity of G-N7 may be explained by variation of the π-stacking interaction between base residues along the double helix. The reaction mixtures containing platinated 3′-G and 5′-G fractions were separated by HPLC. Since the duplexes are self-complementary, the platinated single strands were readily annealed to duplexes with two-fold symmetry and analyzed by 2D [^{1}H, ^{1}H] NOESY NMR spectroscopy. Unexpectedly, the 5′-G-H8 resonance signals of both 5′-G and 3′-G platinated duplexes showed large downfield shifts in the range $\delta = 0.3 - 0.6$ ppm, while the 3′-G-H8 resonance signals in both cases exhibited no, or only slight, upfield shifts. Resonance signals for several other protons in the central region undergo large chemical shift variations induced by platination, indicating that monofunctional binding to DNA leads to appreciable conformational changes.

Keywords: antitumor agents · DNA recognition · NMR spectroscopy · oligonucleotides · platinum

Introduction

Large variations in the efficacy of anticancer platinum drugs are exhibited depending on the type of malignancy. This may be related to differences in the genetic expression, and it is tempting to speculate that the drugs may bind to DNA in a sequence-selective manner. A long-term goal is to design metal complexes that can bind selectively to chosen sequences of DNA. Previously, a general selectivity pattern for 3d transition-metal binding to the guanine residues in double-helical oligonucleotides was proposed based on proton NMR line-broadening studies.[1, 2] The affinity of transition-metal ions for the nitrogen N7 of the G residue on the 5′-side in a double-helical DNA sequence was shown to follow the order: 5′-GG > GA > GT ≫ GC. Surprisingly, the adjacent residue (X) on the 5′-side (5′-XGG) was found to exert a negligible influence on the selectivity. This sequence selectivity is *not* observed for single-stranded oligonucleotides (unpublished results). Photoinduced DNA cleavage experiments by Saito et al.[3] have shown that the sites in B-form DNA most susceptible toward one-electron oxidation are 5′-residues in 5′-GG-3′ steps. This finding supports our proposed selectivity rule, which is based on NMR experiments. It is apparent that adjacent residues exert a minor influence.

Attempts to explain sequence-selectivity by variation in molecular electrostatic potentials (MEPs) along the duplex using the method of Pullman et al.[4] were unsuccessful. A simple electrostatic interaction between a positive metal ion and the most negative base residue does not fully explain the

[a] Prof. Dr. E. Sletten, J. Vinje
Department of Chemistry
University of Bergen
Allègt. 41
5007 Bergen (Norway)
Fax: (+47) 55-589-490
E-mail: einar.sletten@kj.uib.no

[b] Dr. J. A. Parkinson
Department of Pure and Applied Chemistry
University of Strathclyde (UK)

[c] Prof. Dr. P. J. Sadler
School of Chemistry
University of Edinburgh (UK)

[d] Prof. Dr. T. Brown
Biological and Medical Sciences Building
University of Southampton (UK)

Supporting information for this article is available on the WWW under http://www.chemeuj.org or from the author.

  0947-6539/03/0907-1620 $ 20.00+.50/0

experimental results obtained by photochemical cleavage studies, paramagnetic and chemical shift measurements, and reaction kinetics. On the other hand, ab initio calculations of the highest occupied molecular orbitals (HOMOs) of stacked GG doublets in 5-mer duplexes partly support the selectivity rule based on NMR data.[5] In these calculations, the sugar backbones of the B-form duplex were removed from the coordinate file and replaced by methyl groups, keeping the positions of all other atoms fixed. Also, DNA cleavage by cobalt-mediated guanine oxidation correlated well with calculated HOMOs, and this implies that the Co^{II} ion coordinates more strongly to the G residue that has a large HOMO.[5] Consequently, the sequence selectivity of G-N7 metal ion binding, which is obtained from ^{1}H NMR studies, would directly reflect the HOMO distribution in G-containing sequences. Feigon et al.[6] have recently reported that AT-rich sequences can also localize monovalent and divalent cations in a sequence-specific manner. They conclude that the wide and very electronegative minor groove, as found in T_4A_4, provides an excellent site for divalent cation localization, while the narrow minor groove of A_4T_4 is not nearly as favorable.

Numerous publications have dealt with the binding pattern of *cis*-platinum anticancer drugs and the possibility of sequence-selective binding to DNA (see a recent review[7]). One of the first studies on this topic involved enzymatic digestion of DNA platinated by using the well known anticancer drug cisplatin (*cis*-$[PtCl_2(NH_3)_2]$).[8] HPLC analysis of the cleavage products showed that cisplatin forms chelates spanning G and/or A residues with the following populations: Pt-GG (65%), Pt-AG (25%) , Pt-GA (0%). Apparently, the rule of sequence selectivity, which was proposed for labile metal ion complexes and which is based on ^{1}H NMR and photochemical cleavage studies, does not apply to nonlabile platinum complexes. However, the mechanism of chelate formation does not necessarily follow the sequence selectivity of the initial formation of monofunctional adducts. The fact that the 5′-monoadducts are formed more rapidly and chelate more slowly than the 3′-monoadducts may reflect the inherently greater reactivity of the 5′-G compared to the 3′-G. The common view is that the monoaqua species of cisplatin makes the initial attack on DNA bases, although recent results have led Chottard and co-workers to suggest that cisplatin may undergo double hydrolysis before reacting with DNA.[9]

In most reported studies on the kinetics of monofunctional platination reactions of single- and double-stranded oligonucleotides, both NMR spectroscopic and chromatographic methods have been used to determine kinetic parameters.[10] Reactions that involve bifunctional platinum complexes have usually been carried out with single-stranded oligonucleotides. In these reactions, an initial monofunctional adduct is formed that subsequently ring-closes to form a bifunctional chelate. The proposed selectivity rule is expected to be valid only for adduct formation involving duplexes. In a reaction between ^{15} N-labeled $[PtCl(dien)]^+$ and a single-stranded 14-mer d(A-T-A-C-A-**T-G-G-T-**A-C-A-T-A), little kinetic preference for platination of either 5′-G or 3′-G sites was observed, while the single-stranded 8-mer d(A-T-A-C-A-**T-G-G**) showed a distinct preference for 5′-G platination.[10b] Chottard and co-workers, who used hairpin-forming oligomers as duplex models, concluded that the selectivity for monofunctional attack by Pt^{II} on 5′- and 3′-G residues is dependent on the ligand in the *trans* position (e.g., Cl^-, H_2O, OH^-, NH_3).[9a] Quite recently, the same group proposed an interesting new model for sequence-selective binding of cisplatin to DNA duplexes, involving a combination of molecular electrostatic potentials and N7 accessibility.[9b] In a study on selectivity of adduct formation between ^{15}N-cisplatin and 14-mer duplexes containing central -AGT- and -GAT- residues, respectively, Hambley and co-workers concluded that "the purine base on the 3′-side of the pair exerts substantially greater influence on the rate of binding at the 5′-base than does the 5′-base on the rate of binding at the 3′-base".[10d] However, monofunctional binding of cisplatin to the -TGAT- sequence was found to be approximately an order of magnitude slower than binding to -TAGT- sequences, a result which does not agree with the proposed selectivity rule for labile metal ion complexes. Recently, Hambley has summarized the present status on platinum binding to DNA.[11]

Herein we present the results of sequence-selective, monofunctional binding of both labile $(Mn(aq)^{2+}$ and $Zn(aq)^{2+})$ and nonlabile ($[PtCl(dien)]^+$) ions to double-helical DNA oligonucleotides. The studies include kinetic analyses of reactions between ^{15}N-labeled $[PtCl(dien)]^+$ and two 12-mer and one 10-mer palindrome sequences where the central parts differ in the following way: -GGTA-, -GGAT-, -GGCC-. In addition, the preferred binding sites for the metal ions Mn^{2+} and Zn^{2+}, which form labile adducts, have been determined. The results are discussed in relation to ab initio calculations of HOMOs of several G-containing 5-mer duplexes with B-form geometry published by Saito et al.[5b]

Experimental Section

Materials: [^{15}N]-labeled diethylenetriamine was synthesized according to the reported procedure, and [PtCl(^{15}N-dien)]Cl was prepared according to the literature method for the unlabeled complex.[12, 13] The two dodecamers $d(TATGGTACCATA)_2$ I and $d(TATGGATCCATA)_2$ II were purchased from Oswel DNA Service (Southampton, UK) as HPLC-purified oligonucleotides. The decamer $d(TATGGCCATA)_2$ III was obtained from DNA Technology A/S (Aarhus, DK) as the crude product from ethanol precipitation. The chemicals used for HPLC purification: acetonitrile, triethylammonium acetate buffer (made from equimolar amounts of triethylamine and acetic acid), sodium hydrogen phosphate, NaCl and NaOH were purchased from Baker. Sodium perchlorate and sodium dihydrogen phosphate were from Merck. The metal salt $MnCl_2$ was from Baker, and $ZnCl_2$ was from Aldrich (99.999% purity, to minimize the level of paramagnetic metal ion impurities).

NMR spectroscopy: NMR spectra were recorded on the following instruments: Bruker DRX-600 (Bergen) and Varian ^{Unity}*INOVA*-600 and Bruker DMX-500 (Edinburgh). Each instrument was fitted with a pulsed gradient module and a 5 mm inverse probehead. The instruments were used for the acquisition of 2D [^{1}H, ^{15}N] HSQC/HMQC, 2D [^{1}H, ^{1}H] NOESY and 1D ^{1}H NMR spectra. A dpfgsew5 pulse sequence was used to supress water in 1D ^{1}H and 2D [^{1}H, ^{1}H] NOESY NMR spectra recorded in H_2O.[14, 15] A presaturation pulse was used to suppress water in 1D ^{1}H NMR spectra of samples dissolved in D_2O. The spectral width used for 1D ^{1}H and 2D [^{1}H, ^{1}H] NOESY NMR data sets was 6010 Hz for samples dissolved in D_2O and 12019 Hz for samples in H_2O. The 2D [^{1}H, ^{1}H] NOESY NMR spectra were recorded in a phase-sensitive mode using the States-TPPI quadrature

  0947-6539/03/0907-1621 $ 20.00+.50/0

detection scheme.[16] A total of 2048 complex points in t_2 were collected for each of 512 or 1024 t_1 increments. The number of transients were averaged for each increment and the relaxation delays were adjusted for the concentration of the sample. The 2D [^{1}H, ^{15}N] HMQC and [^{1}H, ^{15}N] HSQC NMR spectra were phased with the Echo/Antiecho-TPPI quadrature detection scheme. Pulsed field gradients were employed to select the proper coherence and the ^{15}N spins were decoupled during acquisition. No extra pulse sequence was required to suppress water in HMQC spectra (pulse sequence of Palmer et al.[17]) and HSQC (pulse sequence of Stonehouse et al.[18]) acquired in H_2O. The HMQC and HSQC NMR spectra were optimized for $^1J_{N,H} = 72$ Hz.

The parameters for the HMQC experiments were as follows: spectral width in F1, 3345 Hz; in F2, 4195 Hz; 2048 complex points in each FID in t_2, 64 increments in t_1; four transients were averaged for each increment in the beginning of the reaction, this was gradually increased to 32 transients. A relaxation delay of 2 s was used. The temperature during data acquisition was in the range 273–310 K and was dependent on the type of experiment (^{15}N kinetics, 2D [^{1}H, ^{1}H] NOESY, 1D ^{1}H, line broadening and T_1 measurements). The ^{1}H chemical shifts were referenced to TSP through the HDO resonance signal. An external sample of ^{15}N-labeled NH_4Cl (1 M) in HCl (1 M) was used as external reference for ^{15}N chemical shifts.

1D ^{1}H, 2D [^{1}H, ^{1}H] NOESY and 2D [^{1}H, ^{15}N] HMQC NMR data were processed using the program XWIN-NMR Version 2.6. Data collected for T_1 and T_2 measurements were processed using the program 1D WIN-NMR 5.1. The apodization function used in both dimensions for the 2D data was a pure squared-cosine-bell, and an exponential window function with a line-broadening of 1–5 Hz was applied to the 1D ^{1}H FIDs. The t_1 FIDs in the 2D NMR data sets were linearly predicted to four times their original value, except for FIDs that were recorded with 1024 increments in t_1, which were linearly predicted to 2048 data points.

HPLC oligo purification and separation of reaction mixtures: NMR sample purification was carried out with a Waters 626 LC instrument using Millennium 32 software. The separations were carried out at ambient temperature with a detection wavelength of 260 nm. The dodecamer I was first run through a column (length: 7 cm) filled with the strongly acidic cation exchange resin Dowex-50W (Sigma), then through a column (length: 10 cm) that contained Sephadex G-25 (Pharmacia Biotech). Final purification was carried out on a column (length: 6 cm) that was packed with Chelex resin (Biorad) to remove paramagnetic impurities. Oligonucleotides I and II, which were purchased as HPLC-purified sodium salts, contained traces of paramagnetic impurities that gave rise to appreciable line broadening of the 5′G-H8 protons due to sequence-selective binding of trace paramagnetic ions to G-N7. Chelex resin treatment effectively reduced the 5′-G-H8 line widths to a half-height almost equal to that of the 3′-G-H8 signal. The decamer III was purified by HPLC on a MonoQ HR 10/10 (Pharmacia Biotech) column with the eluents A: 10 mM NaOH, 0.3 M NaCl, pH 12.5; B: 10 mM NaOH, 1.0 M NaCl, pH 12.5. A 60 min linear gradient run from 0% B to 70% B was applied. The samples collected from the separation were immediately neutralized with a small amount of $NaH_2PO_4 \cdot H_2O$ present in the sample collection vessel. The decamer sample was then desalted on a LiChrospher 100 RP-18 column (250 × 4 mm ID, 5 μm, Merck, D). The eluents were A: 5% acetonitrile and 15 mM triethylammonium acetate (TEAA) pH 7.2; B: 70% acetonitrile and 15 mM TEAA, pH 7.2. A 30 min linear gradient from 0% to 15% B was applied. TEAA and acetonitrile were removed by freeze-drying the sample twice, once at pH 12 and once at pH 3. The purified oligonucleotides I, II and III were dissolved in 90% H_2O and 10% D_2O with a salt concentration of 0.1 M $NaClO_4$, pH 6–7. pH values were adjusted with 0.1–1.0 M $HClO_4$ or NaOH, and determined with a Corning 240 pH meter and an Aldrich microcombination electrode, which had been calibrated at pH values of 4, 7, and 10. The mixtures containing the Pt(dien)/duplex reaction products were separated on a MonoQ HR 10/10 (Pharmacia Biotec) column using the same eluents as for the purification of III but with different gradients to optimize resolution. The reaction mixture of I and [Pt(dien)] was separated by a 40 min elution with 70% A and 30% B followed by 20% A and 80% B for 15 min. The products of II were separated with a linear graddient from 35% B to 65% B for 30 min, and for III were separated by 75% A and 25% B for 27 min and then 30% A and 70% B for 14 min.

Mn^{II} and Zn^{II} titrations of duplexes, -GGTA- , -GGAT-, -GGCC-: Mn^{II} and Zn^{II} titrations of the oligonucleotides were carried out in NMR tubes by addition of aliquots of metal salt solutions with a micropipette. The samples of the oligomers were dissolved in D_2O when titrated with $MnCl_2$ and in H_2O when titrated with $ZnCl_2$. The pH of the samples was 6 and the sodium perchlorate concentration was 100 mM. The concentration of metal ions was increased in increments to maximum r values (r = [metal]/[duplex DNA]) in the range 1×10^{-4}–2×10^{-3} for the paramagnetic Mn^{II} system, and 0.1–13 for the diamagnetic Zn^{II} system.

Reaction of duplexes -GGTA- , -GGAT-, -GGCC- with [PtCl(^{15}N -dien)]$^+$: The reactions between [PtCl(^{15}N -dien)]$^+$ and I and II, respectively, were monitored by 2D [^{1}H, ^{15}N] HSQC NMR spectroscopy at T = 288 K. Duplex I and Pt(dien) were mixed in equimolar amounts in $NaClO_4$ (0.1 M) to an initial concentration of 0.8 mM at pH 6. After the reactants were mixed in the NMR tube, the first HSQC NMR spectrum was recorded after 20 min and subsequently after every 20 min for the next two hours followed by longer intervals for the next 10 h. Peak volumes in the 2D [^{1}H, ^{15}N] HSQC 2D NMR spectra were measured by using integration routines in the NMR software. The same procedure was followed for kinetic studies of II with the exception of somewhat higher initial sample concentration (1.1 mM) in the reaction mixtures. For duplex III HMQC spectra were recorded (Bergen) with a concentration of ≈1.3 mM in duplex and slight excess of Pt(dien). Typical spectra demonstrating the variation in intensities for the NH and NH_2 signals of Pt(dien) are shown for I after 30 min and 4 h, respectively (Figure 1).

The reaction products from the platination of I, II, and III were separated on a MonoQ column ≈24 h after the reaction start time. Chromatograms (Figure 2) show three main peaks with increasing elution times: the 5′-G and 3′-G platinated nucleotides, and free nucleotide, respectively. The reaction mixtures of I and II were analyzed again by HPLC a month later after storage of samples at 278 K and, surprisingly, the relative amounts of 3′ and 5′-platinated oligos had changed dramatically (Supporting Information: Figure S1). The amounts of 3′- and 5′-platinated species have equalized for seqence I and are reversed for sequence II. Evidently isomerization has taken place through the rupture of Pt–N7 bonds. New Pt–N7 bonds are formed in more stable monofunctional adducts.

HPLC fractions were desalted by using a NAP-10 column (Pharmacia Biotech) and eluted with sodium phosphate buffer (10 mM, pH 6.6). The volume of each eluted sample was 1.5 mL. Finally, the samples were

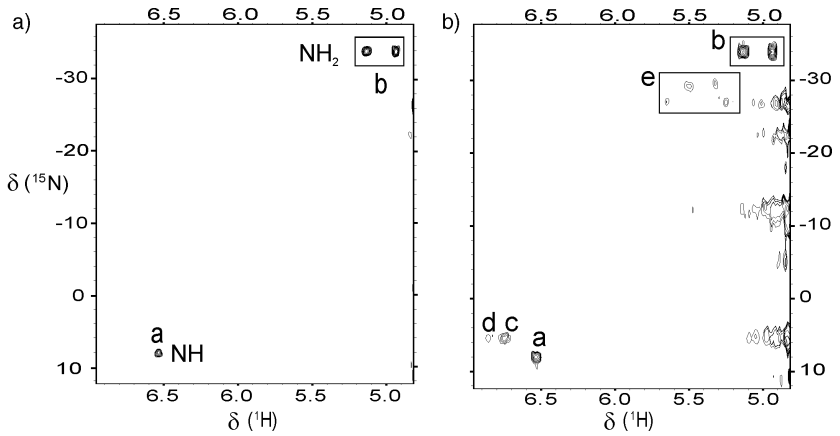

Figure 1. Typical 2D [^{1}H, ^{15}N] HMQC NMR spectra for the reaction between duplex I [d(TATGGTACCATA)]$_2$ and ^{15}N-labeled [PtCl(dien)]$^+$: a) after 30 min; b) after 4 h. Peak a is assigned to Pt-NH, and peaks b to Pt-NH_2 of free Pt(dien). Peaks c and d are assigned to Pt–NH in Pt(dien) adducts Pt-5′-G and Pt–3′-G, respectively, and peaks e represent Pt–NH_2 groups of both Pt–5′-G and Pt–3′-G adducts.

0947-6539/03/0907-1622 $ 20.00+.50/0 *Chem. Eur. J.* **2003**, *9*, No. 7

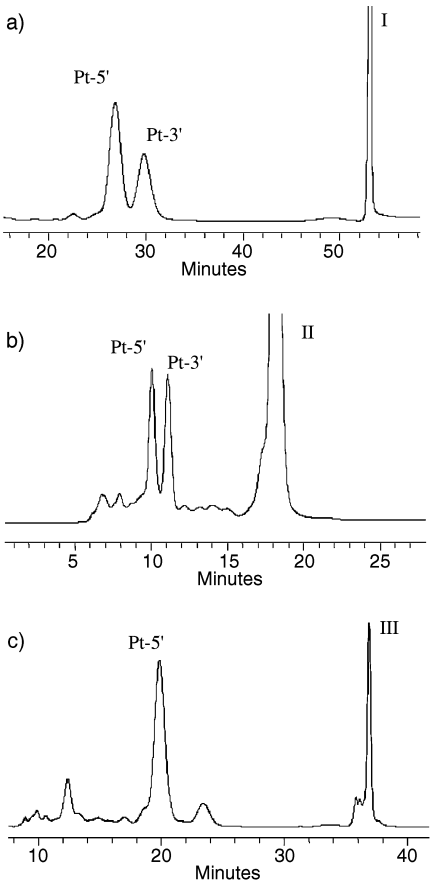

Figure 2. Chromatograms for products from the reaction between $[PtCl(dien)]^+$ and DNA oligonucleotides: a) -GGTA- I; b) -GGAT- II; c) -GGCC- III. The HPLC fractions were collected ≈24 h after the reaction start.

lyophilized and dissolved in 500 μL deionized water that contained $NaClO_4$ (100 mM), D_2O (10%), and sodium phosphate buffer (30 mM). The pH values of the NMR samples were in the range 5.7–6.3.

Data analysis: Rate constants for the reactions were determined by a nonlinear optimization procedure using the program SCIENTIST.[19] The data were fitted using first- and second-order rate equations (see Supporting Information). The extent of hydrolysis of $[PtCl(^{15}N\text{-dien})]^+$ is limited by the relatively high chloride anation rate constant.[20] Thus, the concentration of the aqua complex was too low to be detected, but was estimated from the hydrolysis data.

Results

Proton assignments of the duplexes: The dodecamers $[d(TATGGTACCATA)]_2$ (I), $[d(TATGGATCCATA)]_2$ (II), and the decamer $[d(TATGGCCATA)]_2$ (III) are self-complementary, and the numbering scheme is as, for example, III: 5′-$d(T_1A_2T_3G_4G_5C_6C_7A_8T_9A_{10})$-3′. The proton resonance signals of these sequences were assigned by using the well-known method of sequential connectivity of NOESY cross-peaks for right-handed double-helical DNA. The magnitude of the cross-peaks in the NOESY maps for all three duplexes indicated normal B-form geometry. The spectra of the imino region exhibited the expected Watson–Crick thymine and guanine imino signals (data not shown). As usual, terminal imino signals were found to be very broad, even at low temperature, due to NH exchange with bulk water ("fraying"). Complete assignments of the exchangeable and non-exchangeable proton resonance signals for duplex I are listed in the Supporting information (Table S1).

Mn^{2+} titration: The effects of adding paramagnetic Mn^{2+} ions to aqueous solutions of DNA fragments were monitored by observing the decrease in spin–lattice (T_1) and spin–spin (T_2) relaxation times for protons close to the metal centers. Paramagnetic metal ions may be classified according to their electronic correlation times, that is as relaxation probes that give rise to broad lines or as paramagnetic shift probes with less line-broadening. Manganese(II) is a typical relaxation probe with an estimated electronic relaxation time ($t_s = T_{1e} \approx T_{2e}$) of 10^{-8}–10^{-9} s. Line-broadening is expressed as the line-width at half-height as a function of metal concentration. In kinetically labile metal complexes at low metal-to-nucleotide ratios, paramagnetic shift effects are difficult to detect. In this case geometric information about metal binding sites is most effectively obtained by measuring proton spin–spin (T_2) and spin–lattice relaxation times (T_1). Of special interest is the effect on the G-H8 protons that are adjacent to the expected N7 binding site of guanine residues.

Titration of the -G_4G_5TA- duplex showed a clear preference for Mn^{2+} binding to the 5′- G_4 residue, as demonstrated by the plot of line-broadening versus $r = [Mn^{2+}]/[duplex]$ (Figure 3a). A distinct selectivity pattern emerges, in which the H8 on 5′-G is more strongly influenced than that on 3′-G. The adenine A_{12}-H8 signal, which is plotted as a reference, is not influenced by the paramagnetic ions. The same trend is observed for the measured spin–lattice relaxation times (T_1) (data not shown).

The Mn^{2+} titration procedure was repeated for duplex -GGAT- II and duplex -GGCC- III, and the plots of line broadening versus r are shown in Figures 3b and 3c, respectively. A comparison of the plots for the three duplexes shows some interesting differences. In all cases 5′-G-H8 exhibits the largest paramagnetic line-broadening. However, the most interesting observation is the variation in line broadening for the 3′-G residues which is seen to follow the trend: 5′-GGA > 5′-GGT > 5′-GGC in qualitative agreement with the selectivity rule that was proposed previously.[1, 2]

Zn^{2+} titration: For this diamagnetic system, the chemical shifts for G-H8 protons were monitored as a function of added zinc salt. In contrast to the paramagnetic Mn^{2+} system, excess Zn^{2+} salt was added to the duplex solutions until an upper limit of metal-ion-induced chemical shift changes was reached. This upper level was observed at $r = [Zn^{2+}]/[duplex] \approx 5$, which corresponds to a $[Zn^{2+}]/[G]$ value of ≈1.2. Plots of chemical shift versus r are shown in Figure 4, and a similar trend to that for the paramagnetic system is observed. The relative chemical shift effects of Zn^{2+} ions on 5′-G-H8 resonance signals are clearly stronger than on the 3′-G-H8 resonance signals.

An accurate determination of Zn/DNA stability constants based on variations in chemical shifts is not possible since this variation is related to two major and several minor binding

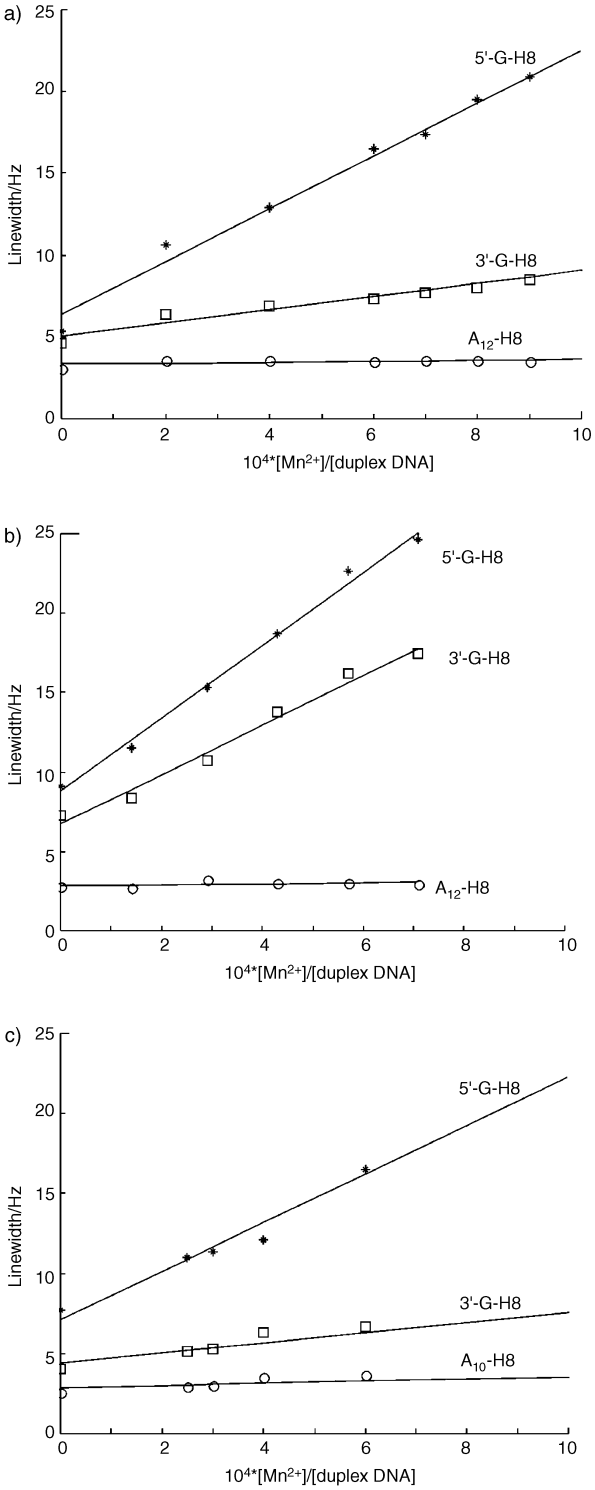

Figure 3. Line-broadening versus Mn^{2+}/duplex ratio (pH = 6) for the H8 resonance signals of 5-G′ (*), 3-G′ (□), and a terminal adenine (○) for comparison. a) d(TATGGTACCATA)$_2$; b) d(TATGGATCCATA)$_2$; c) d(TATGGCCATA)$_2$.

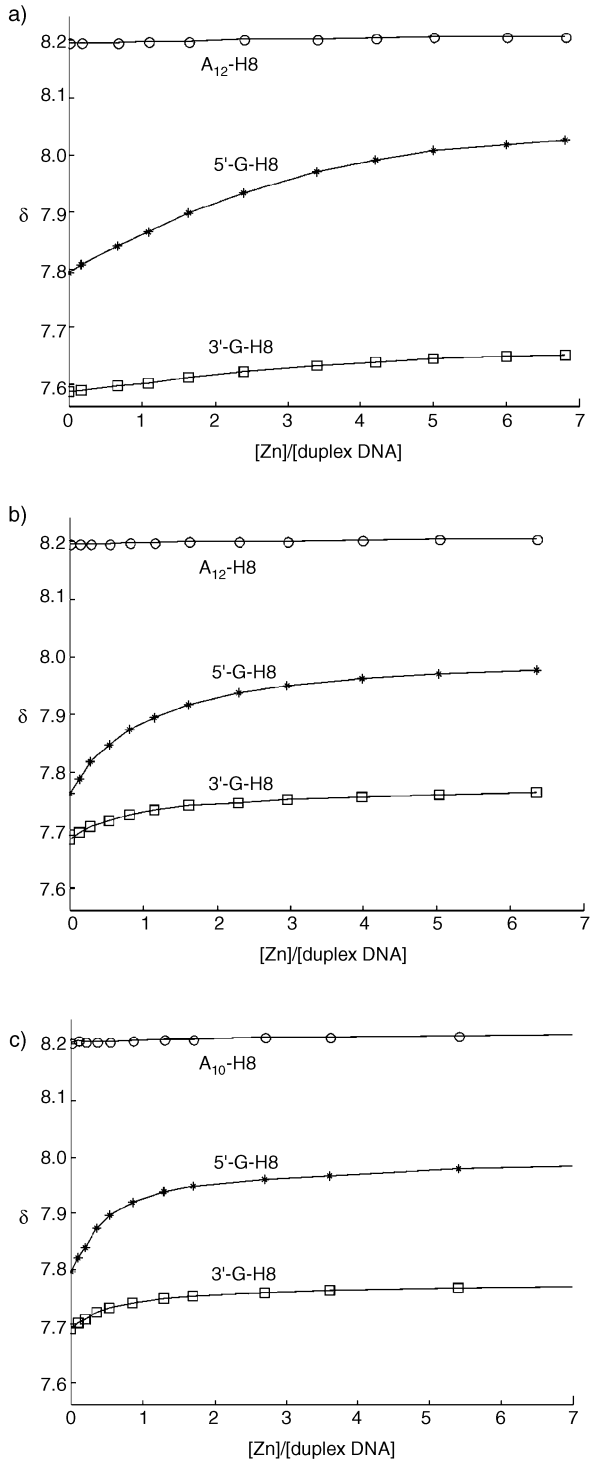

Figure 4. Chemical shift versus Zn^{2+}/duplex ratio plots (pH = 6) for the H8 resonance signals of 5′-G (*), 3′-G (□), and a terminal adenine (○) for comparison. a) d(TATGGTACCATA)$_2$; b) d(TATGGATCCATA)$_2$; c) d(TATGGCCATA)$_2$.

sites. An estimate of the association constants for 5′-G of duplex I using the formula published by Eriksson et al.[21] gave $K = 962$.

[PtCl(^{15}N -dien)]$^+$ duplex kinetics: The reactions between Pt(dien) and each of the three duplexes were monitored by 2D [^{1}H, ^{15}N] HSQC/HMQC NMR spectroscopy for a total of 24 h at 288 K for I and II, and at 298 K for III. Typical [^{1}H, ^{15}N] spectra for the reaction between Pt(dien) and duplex -GGTA- are presented in Figure 1. The development of the cross-peak pattern is shown for $t = 30$ min and $t = 4$ h. Cross-peaks can be assigned to the nonequivalent protons on the two *trans* Pt–NH_2 groups ($\delta(^1H)/\delta(^{15}N)$, 5.1/ – 34.0, 4.9/ – 34.0 ppm), and to Pt–NH *trans* to Cl^- ($\delta(^1H)/\delta(^{15}N)$ chemical shifts of 6.5/

0947-6539/03/0907-1624 $ 20.00+.50/0 *Chem. Eur. J.* **2003**, *9*, No. 7

7.9 ppm). These values are in agreement with earlier assignments for $[PtCl(dien)]^+$ in $NaClO_4$ (0.1 M, pH 5.4), $\delta(^1H)/\delta(^{15}N)$: 5.23/ – 33.8, 5.02/ – 33.8, 6.65/8.1).[22] Previously, 2D [^1H, ^{15}N] HSQC NMR spectra have been reported for a Pt(dien)-platinated 14-mer -GGTA- duplex. This duplex was formed by annealing the 5′-G and 3′-G products that had been separated as single strands by HPLC.[10b] The assignment of 5′- and 3′-platination was not deduced from NMR spectra, but relied on 3′-exonuclease venom phosphodiesterase (VPD) digestion experiments. The corresponding spectra in our systems are quite similar to the composite 5′- and 3′-spectra for the 14-mer duplex. A new set of Pt–NH_2 and Pt–NH cross-peaks emerged during the reaction, while the intensities of the initial cross-peaks diminished. The new Pt–NH cross-peaks represent the dien nitrogen atom *trans* to 5′-G-N7 and 3′-G-N7, respectively. However, from the HSQC/HMQC experiments on the reaction mixture, it is not possible to make an unambiguous assignment. Determination of rate constants was based on the intensities of Pt–NH cross-peaks since the emerging Pt–NH_2 cross-peaks were severely overlapped.

The time courses for reactions of each of the three duplexes are shown in Figure 5. The data were fitted to second-order kinetics using the rate constants for the hydrolysis of $[PtCl(dien)]^+$, which were published by Marti et al.[20].The rate constants, which were determined for the individual guanines, can be accounted for by a two-step kinetic model (Scheme 1).

The first step probably involves an initial, rapid, and reversible formation of the $[PtH_2O(dien)]^{2+}$ complex on the surface of the duplex, followed by the irreversible substitution of H_2O by N7. Direct evidence for preassociation that precedes covalent binding has recently been published by Farrell and co-workers for the reaction of cisplatin with surface-immobilized oligonucleotides.[23] The rate constants are listed in Table 1. The k_5' values are comparable to the rate constant determined by UV spectroscopy for Pt(dien) binding to 5′-GMP (295 K, 100 mM phosphate buffer, pH 5,).[24] For sequence III, the amount of 3′-G-platinated adducts was to small to allow determination of $k_{3'}$. The relative order of $k_5'/k_{3'}$ rate constants (1.2 (GA), 8.6 (GT), and 8 (GC)) follows the same trend as that found for sequence selectivity for adduct formation with labile transition-metal ions.[1, 2] However, the k values differ from those reported by Chottard et al. for cisplatin, which was bound to hairpin-stabilized double-stranded oligonucleotides.[9a, 25] The authors showed that the measured rate constants at pH 4.5 varied considerably according to the type of ligands in the coordination sphere (e.g., Cl, H_2O, OH^-, NH_3). Several factors may account for the apparent discrepancy between our study and that of the Chottard group, for example different pH and ionic strength, difference in ligand geometry between cisplatin and Pt(dien), and the possibility that the geometry of the hairpins may differ somewhat from regular double-helical duplexes. It would be of interest to monitor the kinetics of ^{15}N-labeled cisplatin by 2D (^1H, ^{15}N) NMR spectroscopy and make comparisons with HPLC monitored kinetics.

1D and 2D NMR spectra of $[PtCl(^{15}N\text{-dien})]^+$ duplex solutions: Proton 1D spectra were recorded at 1 h time intervals during the reactions. However, due to the severe overlap of resonance signals from several species, these spectra could not be fully assigned. Proton NOESY NMR data were recorded halfway through and at the end of each reaction. Direct platination of a palindrome duplex at a Pt:G ratio of ≈1:4 yields a mixture of mononuclear G-platinated species. The final NOESY maps are rather complicated and

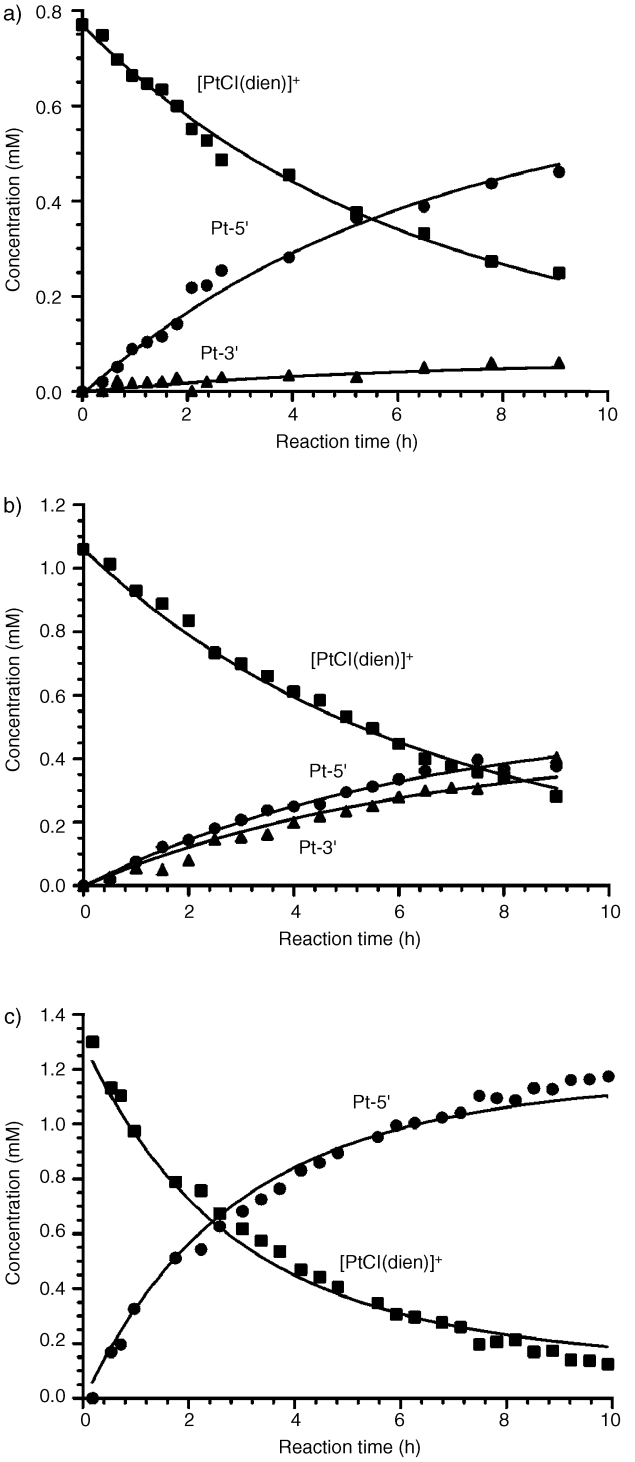

Figure 5. Experimental concentrations (NMR data) and theoretically fitted curves for the reaction between a) 0.8 mM Pt(dien) and 0.8 mM I, b) 1.1 mM Pt(dien) and 1.1 mM II, and c) 1.3 mM Pt(dien) and 1.2 mM III at pH = 6. Symbols: (■) Pt(dien), (●) Pt–G5′, and (▲) Pt–G3′.

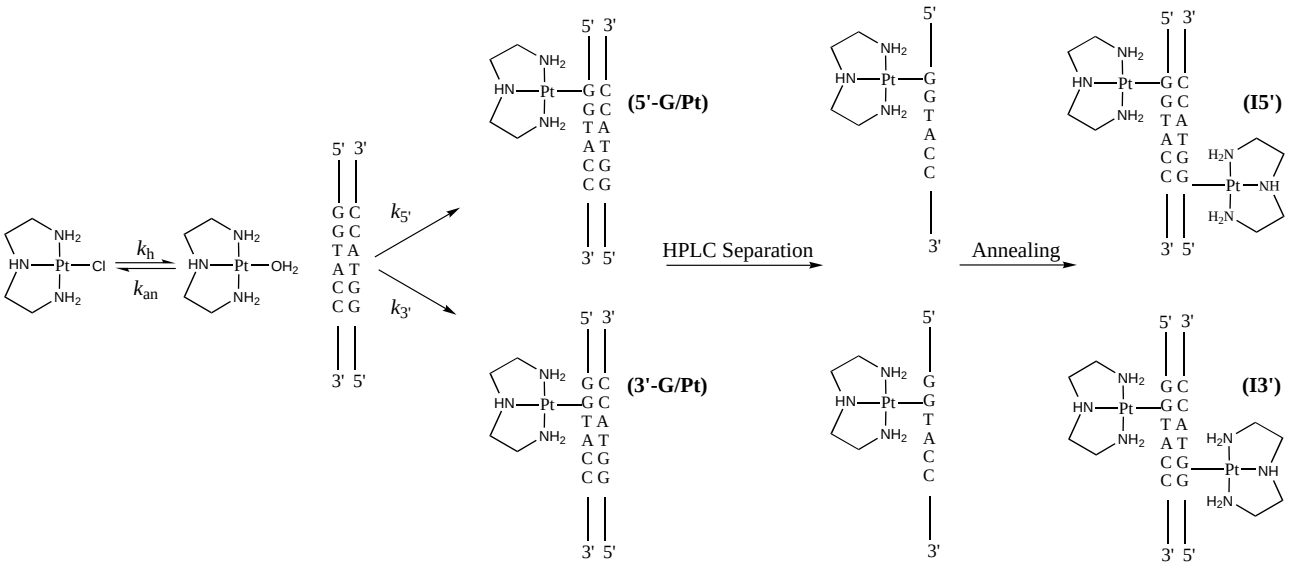

Scheme 1. Reaction pathway of $[PtCl(dien)]^+$ with duplex I, HPLC separation and annealation of the reaction products.

Table 1. Rate constants (standard deviations in parentheses) for reactions of $[PtCl(dien)]^+$ with duplexes I, II, and III (pH 6, in 0.1 M $NaClO_4$).

	$k_{5'}$ [$M^{-1}s^{-1}$]	$k_{3'}$ [$M^{-1}s^{-1}$]	
I	-GGTA-[a]	4.3 (6)	0.5(1)
II	-GGAT-[a]	4.0 (6)	3.4(5)
III	-GGCC-[b]	7.6 (6)	[c]

[a] Temperature = 288 K. [b] Temperature = 298 K. [c] Negligible 3′platination.

contain overlapping signals from unreacted duplex and two major platinated species, as indicated by the HPLC traces of the reaction mixtures (data not shown).

To characterize the reaction products, the HPLC fractions, after appropriate treatment (see above), were transferred to NMR tubes. The imino region of the 1D ^1H NMR spectra showed that the HPLC-isolated platinated single strands had refolded into double-helical palindromes and had retained their twofold symmetry. The largest imino chemical shift change was observed in the spectrum of the -GGTA- duplex, in which T6-H1 in fraction 2 was shifted $\delta = 0.3$ ppm downfield. The concentrations of the samples were relatively low (0.2 – 0.4 mM), but we were still able to trace most of the sequential connectivity in the NOESY spectra (Figure 6). NOE contacts between Pt(dien) amino protons and G-H8 adjacent to the N7 coordination site were assignable, and, most importantly, the two Pt–NH imino signals could be unambiguously assigned to the 5′- and the 3′-G-binding sites, respectively.

Unambiguous assignments of the key base protons were made based on the H6/H8$\cdots$H1′/H5 and H6/H8$\cdots$H2′/H2″ regions of the NOESY map. The chemical shift assignments for 5′-G/Pt and 3′-G/Pt of duplex I are listed in Table S1 in the Supporting Information. A summary of the Pt-induced shifts of G-H8 protons is given in Table 2.

Usually, G-N7 platination produces a significant downfield shift of the ^1H resonance signal for the G-H8 that is adjacent to the binding site, and, in principle, this allows a distinction to be made between 5′-G and 3′-G platination. These downfield shifts mainly reflect the inductive effect of platinum binding, and have been estimated at (0.44 ± 0.01) ppm.[26] The major HPLC fractions are assumed to represent unreacted single strands and monofunctional 5′-G and 3′-G platinated species, respectively. The corresponding G-H8 proton resonance signals are expected to exhibit significant downfield chemical shifts (see above). The spectra of the 5′-G/Pt fraction of each platinated duplex show the following 5′-G-H8 downfield shifts: $\delta = 0.61$ (-GGAT-), 0.62 (-GGTA-), and 0.48 ppm (-GGCC-), which are in agreement with the expected inductive effect of N7 platination, while the 3′-G-H8 proton resonance signals exhibited small upfield shifts of 0.03 – 0.06 ppm. Quite unexpectedly, the spectra of the 3′-G/Pt fraction 2 show almost the same G-H8 shift pattern as that for the 5′-G/Pt fraction: the 5′-G-H8 resonance shifts downfield by $\delta = 0.33$ and 0.32 ppm for the -GGAT and -GGTA- duplexes, respectively, while the 3′-G-H8 proton shifts are practically unaffected ($\delta = 0.03$ and 0.00 ppm) despite Pt binding to the 3′-G base. For the -GGCC- duplex, the HPLC fraction was too small (less than 10 % of the total products) to provide spectra with a sufficient signal-to-noise ratio to detect the G-H8 proton signals.

Based on these shift data, the initial interpretation was that both HPLC fractions represent two isomers of 5′-G-platinated species and that no 3′-G-platinated species exists. This conclusion is unlikely in view of previous results which were obtained from numerous platination studies of DNA oligonucleotides (see, for example, ref. [9]). An alternative interpretation is based on the observation of relatively strong NOE contacts between Pt(dien)-NH_2 protons and G-H8 of the platinated residue. In fraction 1 of each duplex, NOE contacts involve 5′-G-H8 as expected and not 3′-G-H8 (Figure 6). In contrast, the spectrum of fraction 2 contains two significant cross-peaks between 3′-G-H8 and Pt–NH_2, while the 5′-G-H8 protons with downfield shifts of ≈ 0.3 ppm have no Pt–NH_2 contacts. This highly unexpected G-H8 shift pattern must be related to unusual (de)shielding effects that are caused by large

0947-6539/03/0907-1626 $ 20.00+.50/0 *Chem. Eur. J.* **2003**, *9*, No. 7

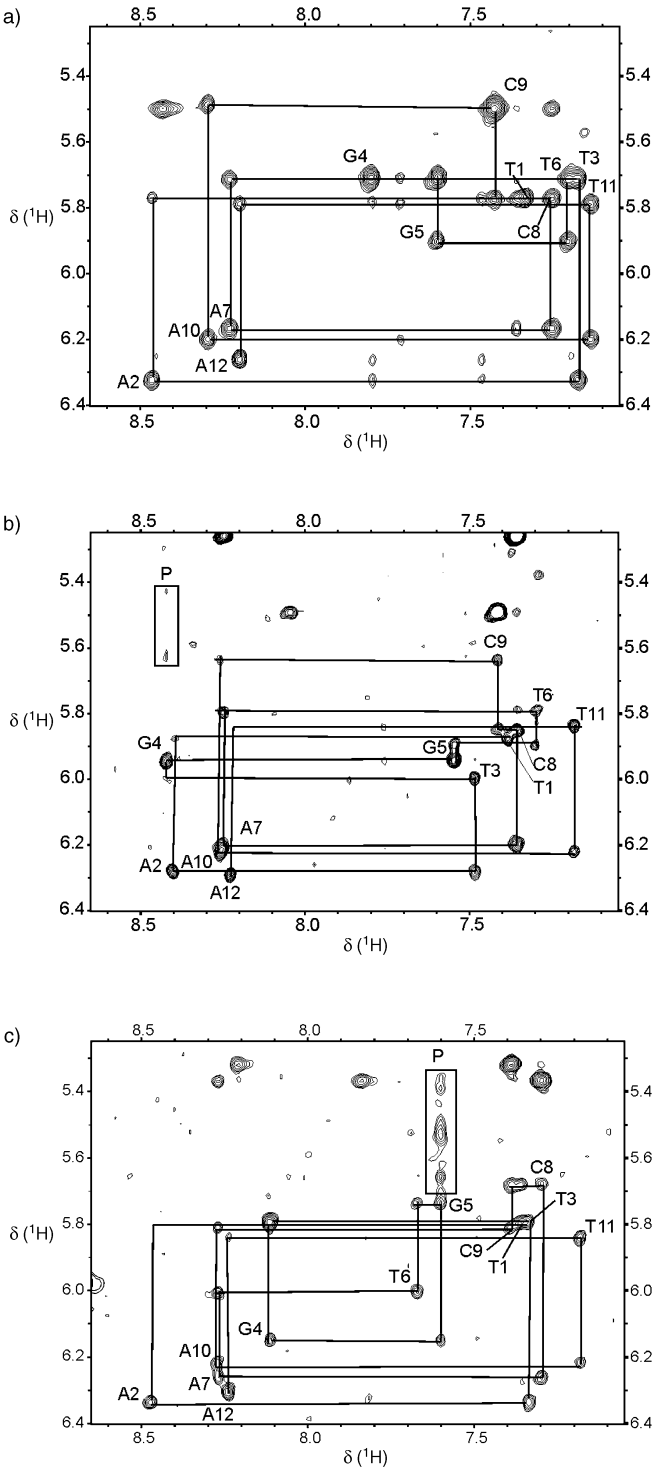

Figure 6. NOESY maps (mixing time 250 ms, T = 285 K, pH = 6) of the H6/H8 ··· H1′/H5 region of duplex I: 5′-[d(TATGGTACCATA)]$_2$. a) Duplex I alone; b) 5′-G-N7/Pt(dien); c) 3′-G-N7/Pt(dien). The signals in box P of b) and c) are cross-peaks between the NH_2 groups of Pt(dien) and H8 of the guanosine to which Pt(dien) is coordinated. In b) the T11/A12 and in c) the T1/A2 cross-peaks are missing, but these are visible at lower temperature (279 K).

structural perturbations of the duplex geometry and are induced by Pt(dien) coordination. These structural changes are seen to induce large chemical shift changes for several protons in the central part of the duplex (Figure 7). Examples

Table 2. G-H8 chemical shift differences between the native duplex and the 5′-Pt/G and 3′-Pt/G fractions of duplex I, II, and III. The asterisks indicate the platinated guanine residue.

		5′-G-H8	3′-G-H8
Pt-G*GTA	I	0.62	– 0.05
Pt-G*GAT	II	0.61	– 0.03
Pt-G*GCC	III	0.48	– 0.09
Pt-GG*TA	I	0.32	0.00
Pt-GG*AT	II	0.33	0.03
Pt-GG*CC	III	[a]	[a]

[a] Negligible platination observed.

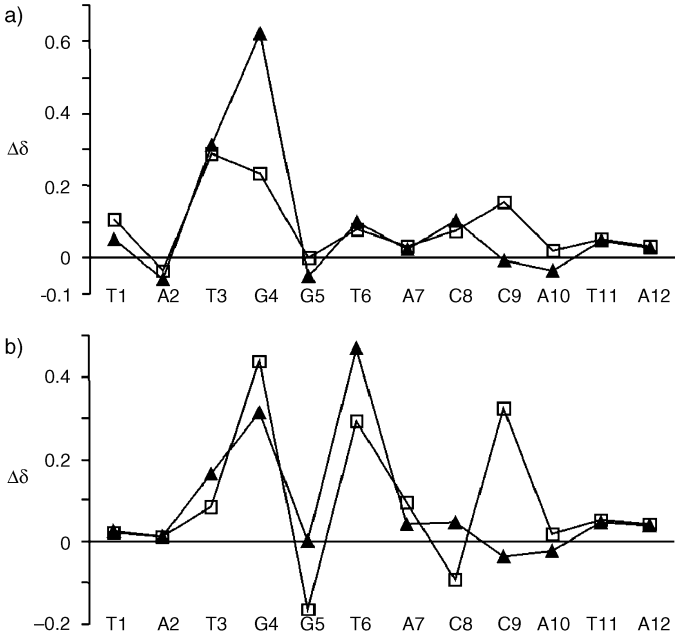

Figure 7. Chemical shift differences for NMR resonance signals of platinated and unplatinated DNA duplex I. a) 5′-G/Pt, b) 3′-G/Pt. Chemical shift differences, $\Delta\delta$, measured as δ(I-Pt) – δI. Symbols: (□) Aromatic H8 or H6 protons and (▲) H1′.

are the large shifts of proton resonance signals for the T6 residue in the -GGTA- duplex (fraction 2): H6 ($\delta = -0.458$), H1′ (−0.293), H2′ (−0.197), H2″ (−0.245), and methyl (0.204 ppm). In this fraction, the adjacent G_5 residue is assumed to be platinated.

Discussion

At present, spectral resolution severely limits the number of residues in oligonucleotides that can be conveniently analyzed by high-field NMR spectroscopy. The use of self-complementary sequences greatly simplifies the spectral analysis due to the twofold symmetry of the duplex. The structure of a short mini-helix is probably sufficiently close to that of native DNA to serve as a realistic model for studying metal-induced local conformational changes, although, end-effects due to "fraying" of the duplex may sometimes influence the binding mode.

The present work has shown that monofunctional, nonlabile platination of double-helical DNA oligonucleotides

using ^{15}N-labeled [PtCl(dien)]$^+$ follows a sequence-selective binding pattern that is similar to that observed for transition-metal ions which form labile adducts. The mode of binding of metal ion complexes to different DNA oligomers is mainly determined by two factors: 1) the nucleophilicity of the binding site, and 2) the coordination geometry of the metal ion complex. Previously some of us have shown that aqua complexes of Mn^{2+}, Co^{2+}, Ni^{2+}, Cu^{2+}, Zn^{2+}, and $Cu(en)^{2+}$ exhibit sequence-selective binding to a series of double-helical oligodeoxyribonucleotides with the following order of affinity for the guanine N7 on the 5′-side: 5′-**G**G > **G**A > **G**T ≫ **G**C.[1, 2] In the present study this selectivity pattern is confirmed for Mn^{2+} and Zn^{2+} adducts of three different duplexes.

Fluctuation in the nucleophilicity of G-N7 is a consequence of the variation of π-stacking interactions between base residues along the duplex. The helical parameters (twist, tilt, roll etc.) are sequence-dependent, and local conformational variations within the B-family of structures have been determined with reasonable precision. For example, the sequence inversion between 5′-AATT- and 5′-TTAA- has been found to change the helical twist, and leads to decreased stacking and consequently to changes in electron-donating properties.[27] Recently, density functional theory (DFT) calculations on Pt/N-containing heterocycles have shown a considerable contribution from π-orbital interactions to the Pt–N bond energy.[28] Experiments on photo-induced DNA cleavage by electron transfer have demonstrated that guanine residues that are located 5′ to an adjacent guanine are the most electron-donating sites in duplex DNA.[5] In photoreaction studies that involved the duplex hexamer 5′-TTGGTA/5′-TACCAA and the duplex heptamer 5′-TTGGGTA/5′-TACCCAA it was found that the reactivity of the G-containing duplex oligomer toward a photosensitizer decreased in the order -GGG- > -GG- > -GA- ≫ GT, -GC-. Recently, ab initio calculations of HOMOs of a wide variety of G-containing 5-mer sequences with B-form duplex geometry were compared to experimental results that were obtained from oxidation of the same sequences with Co^{2+} and benzoyl peroxide.[5b] The distribution of HOMOs along the sequence shown in Table 3 was found to fit the experimentally observed susceptibility to one-electron oxidation and electrophilic attacks at these sites. Qualitatively, these results agree with our rule for sequence-selective binding of metal ions to duplexes based on NMR spectroscopic data. The fact that sequence-selective structural variation in DNA has a profound influence on its electronic structure may also explain conflicting results concerning the conductor and insulator properties of DNA.[29]

Table 3. Distribution of HOMOs (normalized to the largest value) in B-form duplex 5-mers obtained by ab initio calculations (taken from Saito et al. [5b]).

		Upper strand	Lower strand
	5′-G	3′-G	5′-G
5′-T-**G**-**G**-C-T-3′	100	11	
3′-A-C-C-**G**-A-5′			0
5′-T-C-**G**-**G**-T-3′	100	12	
3′-A-**G**-C-C-A-5′			10
5′-A-C-**G**-**G**-T-3′	100	12	
3′-T-**G**-C-C-A-5′			3

In principle, platinum complexes should preferentially attack the more electron-donating sites in DNA duplexes. Of course, steric factors determined by bulky Pt ligands may also play a role. For the most studied platinum complex, cisplatin, the course of the initial attack on DNA is often obscured by subsequent chelate formation. The chelation step, which spans both the 5′-G and the 3′-G residues, is found to proceed much faster for the monofunctional 3′-G species than for the corresponding monofunctional 5′-G species. The fact that monofunctional 5′-adducts are more stable and have longer lifetimes than the corresponding 3′-adducts may explain why AG and not GA adducts of cisplain were observed for calf-thymus DNA.[8] Most platination studies that involve cisplatin have been performed on single-strand DNA followed by annealing to the complementary strand to form a platinated DNA. We have shown (unpublished data) that single-strand metalation does not follow the rule of sequence selectivity, which is apparently, an inherent property of the DNA stacking pattern.

In the present work we find sequence selectivity in the kinetics of monofunctional coordination of Pt(dien) to the G residues in three different duplexes in which the central sequence has been varied systematically. A comparison of reaction rates shows that the selectivity for covalent platination matches that for adducts with labile metal ions. 5′-G in -GGXY- is more reactive than the 3′-G in the order X = A > T ≫ C. However, when the reaction mixtures were aged over several weeks, the relative amounts of 5′ and 3′ HPLC fractions had changed. This was also confirmed by comparison of 2D [^{1}H, ^{15}N] HSQC/HMQC NMR spectra of the aged solutions with those recorded in the initial kinetic experiments. This suggests Pt–N7 bond cleavage and isomerization, which has been observed previously for platinated single-stranded and double-stranded DNA.[10b, 30] Leng and co-workers have suggested a catalytic effect of the DNA double helix to explain the rearrangement that takes place when a stable *trans*-platinated single strand is annealed with its complementary strand.[30g] The rate of the isomerization reaction was found to depend on the nature of the base sequence. The occurrence of Pt–N bond cleavage may influence the results of kinetic analyses that are based on HPLC techniques, in which aliquots of the reaction mixture are collected at several time points and quenched with a large amount of potassium chloride.

It has been demonstrated that formation of monofunctional [PtCl(dien)]$^+$ adducts induces distortions in DNA duplexes.[10g, 30b–d] Reedijk et al.,[30c] in a study on the effect of [PtCl(dien)]$^+$ and [PtCl(NH$_3$)$_3$]$^+$ binding to a nonanucleotide duplex, observed a decrease in the melting temperature by 15–20 K, which is a comparable value to that induced by cisplatin. In a subsequent paper, 1D NMR spectroscopic data suggested conformational changes for the central part of the platinated nonanucleotide duplex.[30d] These results support our conclusions from NOESY NMR spectra which clearly indicate substantial distortion of the central parts of the duplexes due to Pt(dien) platination. The chemical shift pattern of G-H8 protons is unusual and may reflect dramatic

0947-6539/03/0907-1628 $ 20.00+.50/0 *Chem. Eur. J.* **2003**, *9*, No. 7

changes in the ring current effects due to structural distortion. A downfield shift for G-H8 of around 0.5 ppm is usually diagnostic of G-N7 platination.[26] This effect was observed only for 5′-G-N7 platination (≈ -0.6 ppm). In the case of 3′-G-N7 platination, the deshielding effect on 3′-G-H8 is counteracted by an opposite upfield shift induced by variation in ring current effects. Furthermore, when 3′-G-N7 is platinated, the 5′-G-H8 signal moves downfield by $\delta \approx$ 0.3 ppm. Initially, these data were interpreted as representive of two different 5′-G-platinated isomers. Fortunately, an unambiguous assignment can be made to distinguish between 3′-G- and 5′-G-platinated species, which is based on relatively strong NOE cross-peaks that represent contacts between Pt–NH_2 protons and G-H8 of the platinated 3′-G and 5′-G residues, respectively. Variations in the chemical shift pattern for G-H8 of platinated nucleotides have been analyzed in detail by Kozelka, Chottard, and Fouchet[31] and more recently by Marzilli et al.[32] New rules for H8 shifts have been proposed that are based on NMR data and molecular modeling calculations on *cis*-platinated dinucleotides.[33] These cross-linked GG complexes usually have one base canted toward the other, and the H8 signal of the more canted base is further upfield. This effect has been attributed to the ring-current effect of the less canted base, and although dependent on which base is canted, opposite shift effects are found for 5′-G-H8 and 3′-G-H8.[31] In the present system, which involves a doubly platinated helix, similar GG interbase relationships may exist.

Conclusion

An important aim is to provide an experimental method that can predict how different sequences and geometries alter the reactivity of the bases in intact DNA. In this work we have used different NMR spectroscopic techniques to investigate sequence-selective metalation of self-complementary oligodeoxyribonucleotides. Both paramagnetic (Mn^{2+}) and diamagnetic (Zn^{2+}) ions, which form labile adducts with duplexes, as well as $[PtCl(dien)]^+$, which forms nonlabile, monofunctional adducts, have been studied. The results for labile adducts of metal ion/DNA oligomers corroborate previous studies on the interaction between 3d transition metal ions and a series of oligodeoxyribonucleotides.[1, 2]

We have shown that the kinetics of monofunctional binding of divalent platinum to double-helical oligodeoxyribonucleotides follow qualitatively the same selectivity pattern as for labile metal ion adducts. The relative difference in binding affinity between the 3′-G-N7 of 5′-GG*AT- and 5′-GG*CC- is quite dramatic: in the former case the extent of platination of 5′-G is comparable with that of 3′-G, whereas in the latter case there was little 3′-G platination. Calculations published by Saito et al.[5] show that the highest occupied molecular orbital (HOMO) is especially high in energy and concentrated on the 5′-G. As a consequence, one-electron oxidation and electrophilic attack on this G are favored. Structural alterations (e.g., B → Z-form) of the molecular π stack of base pairs represent an unique pathway for site-specific reactions in DNA.

The use of self-complementary sequences has enabled us to separate the species in the reaction mixture and characterize the 5′-Pt and 3′-Pt fractions by 2D NOESY experiments. An unexpected result was the observed chemical shift pattern of the G-H8 protons of the platinated residues of the three duplexes. Usually, platination of G-N7 induces a large downfield shift in the signal from the adjacent G-H8. However, in the spectra of the 3′-G/Pt fractions, no such shift was observed. On the other hand, the 5′-G/Pt fractions gave rise significant downfield shifts for both 5′-G-H8 and 3′-G-H8. This peculiar shift pattern must be related to variation in ring current shifts due to distortion of the central region of the duplexes. The nature of the ligands that are bound to Pt^{II} must play a significant role in determining the distortions in structure of DNA double helices that are induced by platination. If large DNA distortion and protein recognition are major determinants of the efficacy of platinum anticancer drugs, then appropriately designed monofunctional complexes may also be able to fulfill these requirements.

Acknowledgement

We thank the Norwegian Research Council (Grant 135055/432), Wolfson Foundation, Royal Society, BBSRC, The Wellcome Trust and COST Action D20 for their support for this work. We are grateful to Dr. Nils Åge Frøystein for implementing and testing the appropriate pulse programs for recording of HMQC spectra.

[1] N. A. Frøystein, J. T. Davis, B. R. Reid, E. Sletten, *Acta Chem. Scand.* **1993**, *47*, 649–657.
[2] E. Moldrheim, B. Andersen, N. A. Frøystein, E. Sletten, *Inorg. Chim. Acta* **1998**, *273*, 41–46.
[3] a) I. Saito, M. Takayama, H. Sugiyama, K. Nakatani, *J. Am. Chem. Soc.* **1995**, *117*, 6406–6407; b) I. Saito, K. Nakatani, *Bull. Chem. Soc. Jpn.* **1996**, *69*, 3007–3019.
[4] R. Lavery, B. Pullman, *Int. J. Quant. Chem*. **1981**, *20*, 259–272.
[5] a) H. Sugiyama, I. Saito, *J. Am. Chem. Soc.* **1996**, *118*, 7063–7068; b) I. Saito, T. Nakamura, K. Nakatani, *J. Am. Chem. Soc.* **2000**, *122*, 3001–3006.
[6] a) N. V. Hud, V. Sklenar, J. Feigon, *J. Mol. Biol*. **1999**, *286*, 651–660; b) N. V. Hud, J. Feigon, *Biochemistry* **2002**, *41*, 9900–9910.
[7] *Cisplatin – Chemistry and Biochemistry of a Leading Anticancer Drug*, (Ed.: B. Lippert), Wiley-VCH, Weinheim, **1999**.
[8] A. M. Fichtinger-Schepman, J. L. Van der Veer, J. H. J. den Hartog, J. Reedijk, *Biochemistry* **1985**, *24*, 707–713.
[9] a) F. Legendre, V. Monjardet -Bas, J. Kozelka, J. C. Chottard, *Chem. Eur. J.* **2000**, *6*, 2002–2010; b) V. Monjardet-Bas, M. A Elizondo-Riojas, J. C. Chottard, J. Kozelka, Angew. Chem. **2002**, *114* 3124–3127; *Angew. Chem. Int. Ed.* **2002**, 41, 2998–3001.
[10] a) D. P. Bancroft, C. A. Lepre, S. J. Lippard, *J. Am. Chem. Soc*. **1990**, *112*, 6860–6871; b) P. D. Murdoch, Z. J. Guo, J. A. Parkinson, P. J. Sadler, *J. Biol. Inorg. Chem.* **1999**, *4*, 32–38; c) F. Reeder, Z. J. Guo, P. D. Murdoch, A. Corazza, T. W. Hambley, S. J. Berners-Price, J. C. Chottard, P. J. Sadler, *Eur. J. Biochem.* **1997**, *249*, 370–382; d) M. S. Davis, S. J. Berners-Price, T. W. Hambley, *J. Am. Chem. Soc*. **1998**, *120*, 11380–11390; e) S. J. Berners-Price, K. J. Barnham, U. Frey, P. J. Sadler, *Chem. Eur. J.* **1996**, *2*, 1283–1291;f) K. J. Barnham, S. J. Berners-Price, T. A. Frenkiel, U. Frey, P. J. Sadler, *Angew. Chem. Int. Ed.* **1995**, *34*, 1874–1877; g) R. Zaludova, V. Kleinwächter, V. Brabec, *Biophys. Chem*. **1996**, *60*, 135–142.
[11] T. W. Hambley, *J. Chem. Soc. Dalton Trans.* **2001**, 2711–2718.
[12] E. Zang, P. J. Sadler, *Synthesis* **1997**, 410–412.
[13] Z. J. Guo, P. J. Sadler, E. Zang, *Chem. Commun.* **1997**, 27–28.
[14] A. M. Liu, X. Mao, C. Ye, H. Huang, J. K. Nicholson, J. C. Lindon, *J. Magn. Reson*. **1998**, *132*, 125–129.

  0947-6539/03/0907-1629 $ 20.00+.50/0

[15] T-L. Twang, A. J. Shaka, *J. Magn. Reson*. **1995**, *112*, 275 – 279.
[16] D. J. States, R. A. Haberkorn, D. J. Ruben, *J. Magn. Reson*. **1982**, *48*, 286 – 292.
[17] A. G. Palmer III, J. Cavanagh, P. E. Wright, M. Rance, *J. Magn. Reson*. **1991**, *93*, 151 – 170.
[18] J. Stonehouse, G. L. Shaw, J. Keeler, E. D. J. Laue, *J. Magn. Reson*. **1994**, *107*, 178 – 184.
[19] SCIENTIST, version 2.0, Micromath Scientific Software, Salt Lake City.
[20] N. Marti, G. H. B. Hoa, J. Kozelka, *Inorg. Chem. Commun*. **1998**, *1*, 439 – 442.
[21] M. Eriksson, M. Leijon, C. Hiort, B. Norden, A. Graslund, *Biochemistry* **1994**, *33*, 5031 – 5040.
[22] Z. J. Guo, Y. Chen, E. Zang, P. J. Sadler, *J. Chem. Soc. Dalton Trans.* **1997**, 4107 – 4111.
[23] Y. Wang, N Farell, J. D. Burgess, *J. Am. Chem. Soc.* **2001**, *123,* 5576 – 557.
[24] M. I. Djuran, E. L. M. Lempers, J. Reedijk, *Inorg. Chem*. **1991**, *30*, 2648 – 2652.
[25] V. Monjardet-Bas, J. C. Chottard, J. Kozelka, *Chem. Eur. J.* **2002**, *8*, 1144 – 1150.
[26] D. Lemaire, M-H. Fouchet, J. Kozelka, *J. Inorg. Biochem*. **1994**, *53*, 261 – 271.
[27] S-G. Kim, B. R. Reid, *Biochemistry* **1992**, *31*, 12103 – 12116.
[28] D. V. Deubel, *J. Am. Chem. Soc*. **2002**, *124*, 5834 – 5842.
[29] a) T. J Meade in *Metal Ions in Biological Systems*, *Vol. 32* (Eds.: A. Siegel, H. Siegel), Marcel Dekker, New York, **1996**, pp. 453 – 478; b) P. Lincoln, E. Tuite, B. Norden, *J. Am. Chem. Soc*. **1997**, *119*, 1454 – 1455; c) R. E. Holmlin, P. J. Dandliker, J. K. Barton, *Angew. Chem.* **1997**, *109*, 2830 – 2848; *Angew. Chem. Int. Ed. Engl*. **1997**, *36*, 2714 – 2730. d) E. D. A. Stemp, R. E. Holmlin, J. Barton, K. *Inorg. Chim. Acta* **2000**, *297*, 88 – 97.
[30] a) B. Andersen, N. Margiotta, M. Coluccia, G. Natile, E. Sletten, *Met.-Based Drugs* **2000**, *7*, 23 – 32; b) V. Brabec, J. Reedijk, M. Leng, *Biochemistry* **1992**, *31*, 12397 – 12402; c) C. J. van Garderen, H. van den Elst, J. H. van Boom, J. Reedijk, *J. Am. Chem. Soc.* **1989**, *111*, 4123 – 4125; d) C. J. van Garderen, C. Altona, J. Reedijk, *J. Inorg. Chem*. **1990**, *29,* 1481 – 1487; e) R. Dalbies, D. Payet, M. Leng, *Proc. Natl. Acad. Sci*. **1994**, *91*, 8147 – 8151; f) B. Andersen, E. Bernal-Mendez, M. Leng, E. Sletten, *Eur. J. Inorg. Chem.* **2000**, 1201 – 1210; g) M. Boudvillain, R. Dalbies, M. Leng in *Metal Ions in Biological Systems, Vol. 33* (Eds.: A. Siegel, H. Siegel), Marcel Dekker, New York, **1996**, 87 – 104.
[31] J. Kozelka, M. H. Fouchet, J. C. Chottard, *Eur. J. Biochem*. **1992**, *205*, 895 – 906.
[32] S. O. Ano, Z. Kuklenyik, L. G. Marzilli in *Cisplatin – Chemistry and Biochemistry of a Leading Anticancer Drug*, (Ed.: B. Lippert), Wiley-VCH, Weinheim, **1999**, pp. 247 – 291.
[33] L. G. Marzilli, S. O. Ano, F. P. Intini, G. Natile, *J. Am. Chem. Soc*. **1999**, *121*, 9133 – 9142.

Received: November 4, 2002 [F4548]

  0947-6539/03/0907-1630 $ 20.00+.50/0